1 Paleolimnological features of a mega-lake phase in the Makgadikgadi

2 Basin (Kalahari, Botswana) during Marine Isotope Stage 5 inferred

3 from diatoms

4

5 Mareike Schmidt • Markus Fuchs • Andrew C. G. Henderson • Annette Kossler • Melanie J.

6 Leng • Anson W. Mackay • Elisha Shemang • Frank Riedel

7

8 M. Schmidt, A. Kossler, F. Riedel (✉)

9 Institute of Geological Sciences, Freie Universität Berlin, Malteserstr. 74-100, 12249 Berlin,

10 Germany

11 e-mail: paleobio@zedat.fu-berlin.de

12

13 M. Fuchs

14 Department of Geography, Universität Gießen, Senckenbergstr. 1, 35390 Gießen, Germany

15

16 A. C. G. Henderson

17 School of Geography, Politics and Sociology, Newcastle University, Newcastle upon Tyne,

18 NE1 7RU, UK

19

20 M. J. Leng

21 NERC Isotope Geosciences Facility, British Geological Survey, Nottingham NG12 5GG, UK

22 and Centre for Environmental Geochemistry, University of Nottingham, Nottingham NG7

23 2RD, UK

24

25 A. W. Mackay

26 Environmental Change Research Centre, Department of Geography, UCL, Gower Street,

27 London, WC1E 6BT, UK

28

29 E. Shemang

30 Department of Earth and Environmental Sciences, Botswana International University of

31 Science and Technology, Palapye, P. Bag 16, Botswana

32

33 **Keywords**

34

37

38 **Abstract**

39

40 The Makgadikgadi-Okavango-Zambezi basin (MOZB) is a structural depression in the south-

41 western branch of the East African Rift System of the northern and middle Kalahari, central

42 southern Africa. In the present day, the mainly dry subbasins of the MOZB are part of a long-

43 lived lacustrine system that has likely existed since Early Pleistocene and from which an extant

44 freshwater fish radiation emerged seeding all major river systems of southern Africa. During

45 hydrologically favourable periods the subbasins were connected as a single mega-lake termed

46 Lake Palaeo-Makgadikgadi. Previous geomorphological studies and OSL dates have provided

47 evidence for repeated mega-lake periods since approximately 300 ka. The environmental and

48 climatic implications of such large scale late Quaternary lake-level fluctuations are

49 controversial, with the duration of mega-lake phases poorly constrained.

50   Here, we present the first evidence for a Marine Isotope Stage (MIS) 5 mega-lake period

51 (about 935-940 m a.s.l.) reconstructed from a diatom-rich, 30-cm-thick lacustrine sediment

52   section, exposed close to a palaeo-shoreline of the Makgadikgadi Basin. Based upon the

53   environmental setting and in comparison with sedimentation rates of other similar lake

54   environments, we tentatively estimated that the highstand lasted approximately 1 ka during MIS

55   5d-b. The 30-cm section was sampled in 0.5-cm steps. Diatom species diversity ranges from 19

56   to 30 through the section. The dominant species are *Pseudostaurosira brevistriata*, *Rhopalodia*

57   *gibberula*, *Cyclotella meneghiniana* and *Epithemia sorex*. The total of 60 sediment samples

58   provide us with a record at decadal to bi-decadal resolution. Based on diatom assemblages and

59   their oxygen isotope composition ($\delta^{18}O$) we infer an alkaline and mostly oligohaline lake with

60   shallow water conditions prevailing in MIS 5, and is potentially analogous to a Heinrich event.

61   The climate over southern Africa during MIS 5 has been considered very arid but the

62   hydromorphological context of our sediment section indicates that we captured a mega-lake

63   period providing evidence that short-term excursions to significantly higher humidity existed.

64   A hydrologically more favourable environment during MIS 5 than formerly presumed is in line

65   with the early human occupation of the Kalahari.

66

67   **Introduction**

68

69   Geomorphological studies of the northern and middle Kalahari in northern Botswana have

70   provided evidence of a former mega-lake system (Passarge 1904; Grove 1969; Ebert and

71   Hitchcock 1978; Cooke 1979; Heine 1982; Thomas and Shaw 1991; Burrough et al. 2009a;

72   Podgorski et al. 2013; Riedel et al. 2014; Fig. 1), which developed within the Makgadikgadi-

73   Okavango-Zambezi basin (MOZB). The structural depression of the MOZB belongs to the

74   south-western branch of the East African Rift System (Ringrose et al. 2005; Kinabo et al. 2007;

75   Shemang and Molwalefhe 2011; Riedel et al. 2014). Grey and Cooke (1977) termed highstands

76   in this lacustrine system Lake Palaeo-Makgadikgadi (referring to the Makgadikgadi Basin, the

77   largest and deepest of the depressions), which likely comprised of several lacustrine basins (Fig.

78 1) and exhibited a maximum expansion of about 66,000-90,000 km^2 (Eckardt et al. 2008;

79 Podgorski et al. 2013). There is geological and phylogeographical evidence that the mega-lake

80 system may have existed since the Early Pleistocene (Genner et al. 2007; Moore et al. 2012;

81 Riedel et al. 2014; Schultheiß et al. 2014). An OSL (optical stimulated luminescence) date of

82 *c.* 290 ka (Burrough et al. 2009a) provides only a minimum age of the palaeolake system as this

83 is at the limit of the OSL dating technique (Cordier et al. 2012).

84   Burrough et al. (2009a) presented a large number of OSL dates in order to illuminate

85 the chronology of mega-lake periods. Apart from two dates that fall within MIS 8 (*c.* 290 ka

86 and *c.* 270 ka) they dated highstands during MIS 5 to MIS 1. Their OSL samples were taken

87 from palaeo-shorelines of the Makgadikgadi Basin which represents the dominant water body

88 during Lake Palaeo-Makgadikgadi highstands. Burrough et al. (2009a) inferred seven periods

89 of lake highstands in the Makgadikgadi Basin during the past approximately 105 ka. Two of

90 these occurred during MIS 5 (104.6 ± 3.1 ka and 92.2 ± 1.5 ka) and the next youngest one is of

91 MIS 4 age (64.2 ± 2.0 ka).

92   Today, the Makgadikgadi Basin (Fig. 1) is characterized by several salt pans. The largest

93 are the central Ntwetwe Pan (about 4700 km^2) and the eastern Sua Pan (about 3000 km^2), which

94 are occasionally filled with water in modern times, but these temporary infills are not high

95 enough to link the pans together (Riedel et al. 2012). The bottoms of the pans lie generally

96 below an altitude of 950 m a.s.l. (Grove 1969; Grey and Cooke 1977; Cooke 1980; Mallick et

97 al. 1981), with the deepest point (also of the MOZB) located in the northern part of the Sua Pan

98 at an altitude of 890 m a.s.l. (Cooke 1980; Thomas and Shaw 1991; Eckardt et al. 2008).

99   The western margin of the Makgadikgadi Basin is sharply bordered by the prominent

100 Gidikwe Ridge (Fig. 1), which stretches about 250 km from north to south and exhibits a series

101 of palaeo-shorelines. Here, two distinct palaeo-shorelines were determined at an altitude of 945

102 and 936 m a.s.l. (Cooke and Verstappen 1984; Thomas and Shaw 1991; Burrough et al. 2009a,

103 2009b). Lacustrine sediments recorded west to the Gidikwe Ridge (Fig. 1) were interpreted to

104 be of lagoon origin (Cooke 1980; Thomas and Shaw 1991). The backside of the Gidikwe Ridge,

105 however, was considered a second ridge (Moremaoto) by Gumbricht et al. (2001; personal

106 observations FR), delimiting the Makalamabedi Basin (Fig. 1) to the east, which exhibits a

107 curvilinear morphology interpreted as palaeo-shorelines at approximately 930-940 m a.s.l.

108 (Gumbricht et al. 2001; Riedel et al. 2014). Near the Moremaoto Ridge about 2-m-thick diatom-

109 rich sediments (personal observation MS and FR) are exposed, which were originally described

110 in Passarge (1904) who considered an Eemian (MIS 5e) lake period. Shaw et al. (1997) re-

111 studied the diatom-rich sediments, established a MIS 3 age and related them to a lake highstand

112 of the Makgadikgadi Basin. These sediments however are located in the Makalamabedi Basin

113 (Riedel et al. 2014).

114 There are currently no palaeontological records from lacustrine sediments in the MOZB

115 older than MIS 3 (Riedel et al. 2014) that could be used to characterise mega-lake periods.

116 Joyce et al. (2005) concluded an extant cichlid radiation emerged from Lake Palaeo-

117 Makgadikgadi during the Middle Pleistocene seeding all major river systems of southern

118 Africa. These fish require freshwater habitats, which could be sustained over longer periods

119 only when the lake had an outlet (Riedel et al. 2014). The Zambezi, which transverses the

120 northern extension of the lacustrine system, could have acted as an outflow during highstands

121 when all basins where connected into a single mega-lake. It has been suggested that the inflow

122 of the Okavango River, and possibly of the Zambezi, controlled mega-lake periods (Nugent

123 1990). There are, however, several fossil river systems entering the Makgadikgadi Basin

124 (Riedel et al. 2014) of which the Okwa Valley is the largest (Fig. 1). Riedel et al. (2014)

125 suggested that the Okwa River was fully active for the last time during the Last Glacial

126 Maximum and ceased flowing during Heinrich event 1. So far it can only be speculated whether

127 during periods of enhanced Okwa River inflow the Makgadikgadi Basin became exorheic, with

128 an outflow to the west, and freshwater conditions prevailed (Riedel et al. 2014).

129　　　　On the one hand the environmental and climatic implications of such large scale late

130　　Quaternary lake-level fluctuations and the dynamics of aeolian activity are mainly controversial

131　　and on the other hand the discussion has focussed especially on the period MIS 3 to MIS 1

132　　(Street and Grove 1976; van Zinderen Bakker 1976; Heine 1981, 1987, 1988; Stokes et al. 1997;

133　　Gasse et al. 2008; Burrough and Thomas 2009; Burrough et al. 2009a, 2009b; Hürkamp et al.

134　　2011; Riedel et al. 2014). There has been limited work on MIS 5 sediments, and some climate

135　　interpretations do exist although these rely heavily on marine sediments (from off Namibia: Shi

136　　et al. 2001; Stuut et al. 2002) at a low temporal resolution (Urrego et al. 2015). It is noteworthy

137　　that Urrego et al. (2015) reported increased aridity in south-western Africa (neighboring our

138　　study area) during the warmest periods of MIS 5 (5e, 5c, 5a), but they also identified short

139　　increases in humidity during warm-cold and cold-warm transitions. Geyh and Heine (2014)

140　　reported MIS 5 speleothem growth from the Namib Desert. In south-eastern Africa, MIS 5 was

141　　characterized by episodes of extremely arid conditions leading to dramatic lowstands of Lake

142　　Malawi (Cohen et al. 2007; Scholz et al. 2007).

143　　　　　These tropical African MIS 5 "megadroughts" (Scholz et al. 2007) are discussed to have

144　　facilitated human expansions across Africa and ultimately out of Africa (Rito et al. 2013).

145　　Genetic data suggest that anatomically modern humans (Balter 2002) originated in Africa

146　　during MIS 6 (Ingman et al. 2000) and there is archaeological evidence that they populated the

147　　southern tip of Africa as early as ~165 ka (Marean et al. 2007). Genomic diversity of extant

148　　hunter-gatherer populations is in agreement with this early occupation of southern Africa and

149　　tentatively suggests even the orgin of modern humans from this region (Henn et al. 2011).

150　　Symbolic and thus modern behaviour of such southern African human populations may have

151　　first appeared during MIS 5a (Henshilwood et al. 2002) or early MIS 4 (Jacobs and Roberts

152　　2009). In the Kalahari, archaeological sites at the Tsodilo Hills indicate human occupation since

153　　at least 90 ka (Robbins et al. 2016). Burrough (2016) discussed the environmental contributions

154   to early human dispersal in the Kalahari and emphasised the contrast between MIS 5 lake

155   highstands in the Makgadikgadi Basin and extreme lowstands of Lake Malawi.

156   The modern climate setting over semi-arid southern Africa is complex (Peel et al. 2007;

157   Gasse et al. 2008; Chase et al. 2012; Riedel et al. 2014) and comprises moisture transport from

158   the West and East African monsoons (including convective moisture from the Congo Basin) to

159   the Okavango catchment and the Kalahari during austral summer. Rainfall variability in

160   Botswana is described by Batisami and Yarnal (2010).During austral winter, moisture from the

161   south-eastern Atlantic triggers rainfall (mainly) over the Western Cape Province. South-western

162   Indian Ocean (Agulhas Current) derived moisture triggers rainfall over southern Africa mainly

163   during austral summer but also during winter (Chase and Meadows 2007; Gasse et al. 2008;

164   Burrough et al. 2009b; Chase et al. 2012; Urrego et al. 2015).

165   The aim of our study is to reconstruct for the first time the palaeohydrological status of

166   a mega-lake phase (about 66,000-90,000 km^2) in the MOZB, which corresponds to a highstand

167   of at least 936-945 m a.s.l. of Lake Palaeo-Makgadikgadi, by analyzing diatom assemblages

168   and their oxygen isotope composition ($\delta^{18}O_{diatom}$). The mega-lake phase adressed here occurred

169   during MIS 5 and is the first attempt to infer the duration of a mega-lake phase in this region.

170   Our findings contribute to the understanding of phylogeographical patterns and climate

171   evolution of southern Africa.

172

173   Study site

174

175   Our study site (Fig. 1) is located at the Gidikwe Ridge where the ridge is cut by the Boteti River

176   valley forming a 20-22 m deep gorge. Here, a 10-m-thick sedimentary succession was exposed

177   (S20.28672°, E24.26822°), which exhibited 40 cm consolidated, heavily diagenetically altered

178   lacustrine deposits at the base, followed by 9.3 m unfossiliferous, silcrete- and calcrete-rich

179   playa sediments (Riedel et al. 2014). On the top of the succession of sediments, at about 935 m

180   a.s.l., the playa sediments are overlain by a 30-cm-thick unit (Fig. 2), which consists of

181   consolidated, fine-laminated to thin-bedded, finely clastic, light-grey to whitish lacustrine

182   sediments rich in diatoms and deposited during MIS 5 (Riedel et al. 2014). Lithological hiatuses

183   were not identified in the 30-cm unit, suggesting sedimentation was continuous. This sediment

184   unit thins out a few hundred metres west of the section where sandy palaeo-beach features can

185   be found indicating that the former shore was relatively close.

186

187   **Material and Methods**

188

189   Sediment samples

190

191   The 10-m sediment outcrop within the Boteti Gorge at the western margin of the Makgadikgadi

192   Basin (Fig. 1 and 2) was first visited by AK and FR in 2007 and a small number of samples

193   were taken. Samples from a 40-cm-thick unit of white and pale-gray lacustrine sediments at the

194   base of the profile has been strongly affected by diagenesis, and contains only few broken

195   valves of diatoms, while the light-grey to whitish 30-cm-thick deposits at the top of the section

196   (Boteti Top = BT) have abundant diatoms. Although carbonate is contained in BT, remains of

197   ostracod valves were only exceptionally preserved. Except for a few pollen grains, no other

198   fossil remains were identified. When revisiting the section in 2009 samples for OSL dating

199   were taken from the two lacustrine sediment units. MF provided an OSL date suggesting MIS

200   5 age for BT. OSL dating of the 40-cm unit at the base of the Boteti section failed because the

201   OSL signal was close to saturation and therefore at its upper limit.

202   In 2011 the outcrop was revisited for high resolution sampling and a fresh surface was

203   exposed and thoroughly cleaned using spade, saw, knife and brush. The sampling of the

204   relatively hard sediments was done in 0.5-cm increments with a knife from the base to the top

205   of the BT unit. 60 sediment samples of about 60 grams each were taken, sample BT_{diatom}-1

206 corresponding to the lowermost and sample BT_{diatom}-60 to the uppermost layer. In addition,

207 using a saw, a 30x15x15-cm-sediment block was removed covering the complete BT unit in

208 order to obtain suitable material for optical dating. The sawed surfaces did not exhibit cracks

209 through which light could have penetrated into the internal sediments. The block was

210 immediately wrapped with thick black plastic foil and stored in a sealed box.

211

212 OSL dating

213

214 Samples were taken from the lower (BT 1055), middle (BT 1054) and upper part (BT 1052) of

215 the sediment block in the OSL lab of Bayreuth University, Germany. A further sample (BT

216 885) from the middle part of the BT section had been already obtained during field work in

217 2009 (Fig. 2).

218 The coarse grain quartz fraction (90-200 μm) of the sediment samples was used for OSL

219 dating. Luminescence measurements were carried out using a Risø-Reader TL/OSL-DA-15

220 (Bøtter-Jensen 1997), equipped with blue LEDs (470 ± 30 nm) for stimulation, a Thorn-EMI

221 9235QA photomultiplier combined with one 7.5 mm U-340 Hoya filter (transmission 290-370

222 nm) for detection and a $^{90}Y/^{90}Sr$ β-source (8.1 ± 0.6 Gy/min) for artificial irradiation.

223 The equivalent dose (D_e) was determined by applying a single aliquot regenerative

224 (SAR) dose protocol (Murray and Wintle 2000). Shine-down curves were measured for 20 s at

225 elevated temperatures (125°C) after a preheat for 10 s at 220°C and 240°C respectively for the

226 natural and regenerated signals and a cut-heat of 160°C for the test doses. The preheat

227 temperatures were chosen after a preheat plateau test, which indicated that the given dose could

228 be reproduced within a temperature range of 220°C to 240°C.

229 Finally, the D_e was calculated from the integral of the first 0.4 s from the shine-down

230 curves after subtracting the mean background (16-20 s) signal. For each sample, up to 28 small

231 aliquots (steal cups) were measured with 200-500 grains per aliquot. Possible feldspar

232 contamination of the aliquots was checked by stimulating the artificially irradiated samples with

233 infrared (IR-OSL) and detecting in the UV range (290-370 nm). For D_e determination, only

234 those aliquots of a sample were used, which passed the criteria of a recycling ratio of 1 ± 0.1

235 and a recuperation value of $< 5\%$ (Murray and Wintle 2000). The standard error was used as D_e

236 error.

237   The dose rate($\dot{D}$) for OSL age calculation was determined by thick source α-counting

238 and ICP-MS. Cosmic-ray dose rates were calculated according to Prescott and Hutton (1994).

239 The water content of the samples was determined using the average value of the possible water

240 content range, based on the porosity of the samples. An error for the water content value was

241 chosen, which included the possible water content range. The values used for the water content

242 were checked by measuring the in situ water contents of the samples, showing conformity

243 within errors.

244

245 Diatom assemblages

246

247 Diatom extraction and slide preparation for microscopic analyses were carried out following

248 Battarbee et al. (2001). Diatom identification and counting were performed using a Meiji

249 Techno 4000 microscope at 1000x magnification with an oil immersion objective.

250 Approximately 500 diatom valves were counted per sample to ensure that effective numbers of

251 taxa were counted. Diatom relative abundances were plotted using Tilia® (Grimm 1991-2011),

252 and planktonic to benthic ratios calculated according to the formula: $\sum$(planktonic) /

253 $\sum$(planktonic + benthic).

254   For precise identification of the diatom taxa, a Zeiss Supra 40 VP scanning electron

255 microscope (SEM) was additionally used. Diatoms for the SEM analyses were prepared by

256 drying 0.5 ml of the treated sample suspension on a cover slip fixed on a stub. After drying, the

257 diatoms were coated with gold in a sputter coater and then examined with the SEM. Diatom

258   species were identified using, amongst other keys, Krammer (2002), Krammer and Lange-

259   Bertalot (1997, 1999, 2000, 2004), Levkov (2009) and Kusber and Cocquyt (2012). A list of

260   species and their authorities is provided in ESM 1.

261   The ecological preferences of identified diatoms concerning salinity, pH and trophic

262   level were taken from the literature (ESM 2), but are unknown in some taxa. The salinity

263   classification follows Schlungbaum and Baudler (2001): freshwater = < 0.5 psu; oligohaline =

264   0.5 to < 5 psu; mesohaline = 5 to 18 psu; euryhaline = fresh to saltwater, indifferent or non-

265   significant.

266   Ordination analyses were undertaken using Canoco 4.5 (ter Braak and Šmilauer 2002)

267   to reveal major trends in the diatom data. An initial detrended correspondence analysis (DCA)

268   gave an axis 1 gradient of only 0.734, revealing a dataset with very little species turnover, so

269   principal components analysis (PCA) was used instead. Scaling for both samples and species

270   was optimized through symmetric scaling of the ordination scores (Gabriel 2002). Because we

271   have closed relative abundance data, species data were log (x+1) transformed and both species

272   and samples were centred to give a log-linear contrast PCA (Lotter and Birks 1993). To

273   determine if any of the PCA axes were in themselves significant in explaining variation in the

274   diatom data, a broken stick analyses was undertaken (Jollifer 1986). The diatom stratigraphy

275   was zoned using Constrained Incremental Sum of Squares Cluster Analysis (CONISS)

276   according to Grimm (1991-2011).

277

278   Diatom oxygen isotope analysis

279

280   From the 60 BT samples studied in respect of diatom assemblages, alternate samples were

281   analysed for their oxygen isotope composition. Following the protocol established by Morley

282   et al. (2004) the 30 sediment samples for $\delta^{18}O_{diatom}$ analysis underwent chemical digestion using

283   30% H_2O_2 and 5% HCl followed by sieving of samples at 74 µm and 10 µm. Diatoms were

284 then isolated using a combination of differential settling and heavy liquid separation using

285 sodium polytungstate (SPT). The SPT was then washed out of the purified sample using

286 multiple rinses of deionised distilled water, and dried down prior to analysis. Samples were

287 measured using a step-wise fluorination procedure using 6 mg of sample (Leng and Sloane

288 2008) and a Finnigan MAT 253 isotope ratio mass spectrometer. $\delta^{18}O_{diatom}$ were converted to

289 the Vienna Standard Mean Ocean Water (VSMOW) scale using an international laboratory

290 diatom standard (BFC_{mod}) calibrated against NBS28. The methology has been verified through

291 an inter-laboratory calibration exercise (Chapligin et al. 2011). Replicate analyses of sample

292 material from this current study indicating an analytical reproducibility (mean difference) of

293 0.2‰ ($1\sigma = 0.5$, n = 9).

294

295 **Results**

296

297 OSL dating

298

299 The suitability of the quartz extracts for OSL dating was evaluated using a combined preheat

300 plateau and dose-recovery test. In ESM 3c, the result of this test is shown, indicating the given

301 dose of 70.2 Gy could be reproduced within a temperature range of 220°C to 260°C. In addition,

302 ESM 3a shows a typical OSL shine-down curve, displaying a bright OSL signal that is quickly

303 bleached to measurement background. Growth curves could be established with high precision,

304 with recycling ratios of 0.9-1.1 (ESM 3b). Thus, the OSL quartz behavior, the preheat plateau

305 and the dose-recovery tests demonstrate the suitability of the applied SAR protocol.

306   In Table 1, the analytical data for OSL age calculation, including the data for dose rate

307 determination are given. The results of the OSL age calculation ranging from 106.3 ± 7.4 to

308 88.5 ± 5.8 ka indicate the studied section can be assigned to MIS 5. The sample BT 1055 from

309 the lower part of the studied sediment unit (Fig. 2) has an OSL age of 103.4 ± 6.4 ka, the

310   following sample BT 1054 from the middle part of the 30-cm unit (Fig. 2) shows an age of

311   106.3 ± 7.4 ka, which is within errors still consistent with the stratigraphic order. Sample BT

312   1052 from the upper part (Fig. 2) reveals an age of 90.3 ± 9.2 ka. The sample BT 885, which

313   was previously taken in 2009, shows an age of 88.5 ± 5.8 ka and correlates with the result of BT

314   1052 (Table 1).

315

316   Diatom assemblages and $\delta^{18}O_{diatom}$

317

318   The microscopic analyses of the samples reveal the sediments are rich in well-preserved diatom

319   valves (Fig. 3). In total, 50 species could be identified of which 44 species are benthic, that is

320   they prefer littoral rather than planktonic habitats (ESM 1, ESM 22). The number of species per

321   sample ranges from 19 to 30. Generally, most species are represented by a few valves only.

322   Benthic diatoms dominate the whole sequence (70 to 95%), especially in the uppermost

323   sediments, resulting in very low planktonic/benthic ratios (Fig. 4).

324   Using broken stick, only PCA axis 1 showed significant variation. PCA axis 1 sample

325   scores are therefore also plotted against depth in Fig. 4. These data show considerable variation,

326   superimposed on a strong directional change from the base of the sediment unit to about 25 cm,

327   before sample scores decline to the top of the profile. A moderate but significant Pearson

328   product moment correlation coefficient exists between PCA axis 1 sample scores and the P/B

329   ratio ($r = -0.618$; $p = 0.0001$). CONISS has delimited 3 zones (Kala-1 to Kala-3), with major

330   divisions at 13.75 cm and 23.25 cm (Fig. 4).

331   Kala-1: This zone is dominated by *Pseudostaurosira brevistriata* and *Rhopalodia*

332   *gibberula*, although the planktonic *Cyclotella meneghiniana* is also abundant, resulting in

333   highest P/B ratios for the sequence and lowest PCA axis 1 samples scores. *Halamphora*

334   *thermalis* is also relatively common. At this time, $\delta^{18}O_{diatom}$ values increase steadily to their

335   highest values of +34.2‰ at 11.5 cm.

336   Kala-2: This zone is delimited by a small peak in *P. brevistriata*, a P/B minimum and

337   declining $\delta^{18}O_{diatom}$ values. Within this zone, the most notable changes include declining *C.*

338   *meneghiniana* values and increases in *Epithemia sorex.*

339   Kala-3: This zone is delimited by very low P/B ratio values and high PCA axis 1

340   samples, and lowest $\delta^{18}O_{diatom}$ values (+28.2‰ at 23.5 cm). During this zone, *C. meneghiniana*

341   values are generally at their lowest, while *E. sorex* values are at their highest. Towards the top

342   of this zone, P/B ratio values increase slighty, concomitant with declining PCA axis 1 sample

343   scores and increasing $\delta^{18}O_{diatom}$ values to about +31‰.

344   The inferred hydrological parameters (salinity, trophic status, pH) show little variation

345   throughout the palaeolake-phase. Most diatoms are tolerant to salinity fluctuations but about

346   15% of the species of the assemblages reflect oligohaline conditions in zones Kala-1 and -2

347   with an increase to 20% in Kala-3. About 60% of the diatom species indicate eutrophic

348   conditions and 20-30% are nutrient-tolerant. The pH reconstruction indicates alkaline

349   conditions (> 7). Approximately 30-40% of the diatom species require pH values of 7-8 and

350   50-80% of 8-9 with slight decrease of alkalinity during zone Kala-3.

351

352   **Discussion**

353

354   Dating

355

356   Age calculation of mega-lake phases in the MOZB (Fig. 1) have previously been established

357   using a large set of OSL dates from palaeo-shoreline features (Burrough and Thomas 2009;

358   Burrough et al. 2009a, 2009b). In respect of MIS 5, Burrough et al. (2009a) identified two

359   highstands of Lake Palaeo-Makgadikgadi centred at *c.* 105 ka and *c.* 92 ka respectively,

360   analysed as "events of unknown duration" (Burrough et al. 2009b). In contrast to samples

361   obtained from shoreline sediments (Burrough et al. 2009a), which may have been reworked by

362 waves, we dated quartz grains from a low energy aquatic milieu. The fine lamination of the

363 sediments indicates still water conditions below the wave-line and reworking of the sediments

364 can likely be ruled out. The range of our dates, however, shows large uncertainty remains.

365 Considering the uncertainties of the oldest (106.3 ± 7.4 ka) and the youngest age (88.5 ± 5.8

366 ka), the max. range is 113.7-82.7 ka, a period of 31 ka covering roughly MIS 5d-b, and the min.

367 range is 98.9-94.3 ka, a period of 4.6 ka.

368 The range has to be considered in the context of the duration of continuous deposition

369 of 30 cm of lacustrine sediments. In comparision with lake systems showing at least partly

370 similar (palaeo-)environmental settings (Aral Sea: 30 cm ~650 years, Filippov and Riedel 2009;

371 Lake Titicaca: 30 cm ~900-1200 years, Fornace et al. 2014; Tso Moriri, Ladakh, India: 30 cm

372 ~1100 years, Leipe et al. 2014; Lake Kotokel, Buryatia, Russia: 30 cm ~700 years, Kostrova et

373 al. 2016; Lake Teletskoye, Russian Altai: 30 cm ~600 years, Mitrofanova et al. 2016; Lake

374 Van, Turkey: 30 cm ~1000 years, North et al. unpublished data) it can be roughly estimated

375 that the 30-cm sediment unit of the Boteti section had been deposited during a period of

376 approximately 1 ka.

377 It is possible, but not likely that the terminal highstand is not archived in the 30-cm unit.

378 This could be because of potential deflation processes after the lake level had decreased. Once

379 exposed, sediments of such composition usually harden quickly under a (semi-)arid climate and

380 subsequent weathering and erosion processes are limited. This is also due to the fact that under

381 retreating lake levels, aeolian activity is increasing and consolidated lacustrine sediment

382 sequences are often, instead of being deflated, covered by sand (as can be observed across the

383 MOZB), which protects them from erosion. Moreover, the 40-cm-lacustrine-sediment unit at

384 the base of the Boteti section, which is overlain by playa sediments, appears to be complete and

385 provides an independant example of a relatively short lake highstand. We thus can provide at

386 least a first idea how long so-called mega-lake phases may have lasted.

387   The estimation that the 30-cm-sediment unit covers a period of not more than

388   approximately 1 ka allows us to infer a temporal resolution of the analysed samples of 1-2

389   decades. Dating uncertainties remains a major challenge for an accurate reconstruction of

390   environmental dynamics in the Kalahari, and is probably responsible for most of the

391   controversial discussions related to (Street and Grove 1976; Heine 1981, 1987, 1988; Stokes et

392   al. 1997; Gasse et al. 2008; Burrough and Thomas 2009; Burrough et al. 2009a, 2009b; Chase

393   and Brewer 2009; Hürkamp et al. 2011; Riedel et al. 2014; Burrough 2016).

394   Significant uncertainties also exist with respect to measured palaeo-shoreline altitudes.

395   In a number of studies the uncertainty is as high or even higher as the 9 m difference between

396   the 936 and 945 m a.s.l. palaeo-shorelines (Riedel et al. 2014). On the other hand, it is unlikely

397   mega-lake highstands reached the same elevation repeatedly, except in exceptional

398   circumstances. The two different lacustrine sediment units of the Boteti section indicate two

399   lake periods at the same position, which means they are of likely similar extension, although

400   the older highstand is about 9.3 m lower than the younger one. The amount of available water

401   during these two periods may have been similar, pointing at comparable climate settings, but

402   with increased accumulation of sediments in the MOZB raising the lake floor (Haddon and

403   McCarthy 2005). Thus a higher lake level of significant younger age than an earlier lower lake

404   level could have potentially been reached even with less hydrological input.

405

406   Diatom assemblages and $\delta^{18}O_{diatom}$

407

408   The diatom assemblage presented here is very different from contemporary flora found in the

409   fresh, shallow waters of the Okavango Delta (Mackay et al. 2012). The dominance of benthic

410   taxa (Fig. 4) in the BT unit indicates the persistence of shallow water conditions and extensive

411   littoral regions, especially during the terminal stages of sediment accumulation (zone Kala-3).

412   Patrick (1977) described *E. sorex* as an aerophilous species that can persist in environments

413 characterized by desiccation. Therefore, an increase of the abundance of *E. sorex* within the

414 sediments at this time potentially shows a stronger proximity to the shoreline caused by a drop

415 in lake level during this period of inferred lake level decline. The maximum water depth can be

416 calculated in the hydromorphological context to have been a few metres only (max. depth of

417 palaeolake ~50 m). The diatom assemblages reveal changes in lake water depth throughout the

418 record. The significant correlation between PCA axis 1 sample scores and P/B ratio suggests

419 varying water levels influenced diatom composition in the shallow lake waters. What is notable

420 is the period of highest P/B ratio is coincident with increasing $\delta^{18}O_{diatom}$ values (increasing

421 effective moisture), indicative of increasing planktonic habitats in this part of the lake (Fig. 4).

422   These shallow waters were likely freshwater to brackish; qualitative salinity

423 reconstruction indicate oligohaline conditions (0.5 to < 5 psu) persisted during the whole period

424 (Fig. 4). For example, the dominant species *P. brevistriata*, *R. gibberula* and *M. elliptica* have

425 wide salinity tolerances (Caljon and Cocquyt 1992; Krammer and Lange-Bertalot 1999; van

426 Dam et al. 1994; Stachura-Suchoples 2001). *E. sorex* is also described from oligohaline waters

427 (Cholnoky 1968; Patrick 1977; Krammer and Lange-Bertalot 1999; Kelly et al. 2005), while *C.*

428 *meneghiniana* is often found in brackish water (Hecky and Kilham 1973).

429   The qualitative oligohaline salinity reconstruction at the study site does not mean that

430 Lake Palaeo-Makgadikgadi was oligohaline in general but exhibited salinity gradients. Filling

431 up and interconnecting the lacustrine basins to a single lake (Fig. 1) required significant inflow

432 from at least one of the major river systems, either from the Okavango River in the (north-)west

433 or from the Okwa River in the southwest. It also cannot be ruled out that both river systems

434 were active simultaneously. If the Okavango was the main source of hydrological input, the

435 main lacustrine depression of the palaeolake-system, the Makgadikgadi Basin, would have

436 acted as a terminal lake with increasing salinity to the east (Fig. 1). The likely outflow in this

437 scenario would be through the Zambezi valley. Therefore, western lake areas between major

438 inflow and outflow would have been under freshwater conditions. An example of a comparator

439 to this behaviour can be found at extant Bosten Lake, Xinjiang, China, where inflow and

440 outflow are located at the western side of the lake and freshwater conditions prevail only there,

441 while the largest part of the water body is oligohaline (Mischke and Wünnemann 2006; Wufuer

442 et al. 2014; personal observation FR). A second scenario considers the Okwa River the main

443 source of water inflow during the highstand. In this case the Makgadikgadi Basin was exorheic

444 and the study site would have been in proximity to the outflow. In both scenarios freshwater

445 areas are limited, and considering the relatively short period of approximately 1 ka, the mega-

446 lake phase likely did not foster evolutionary radiations of freshwater fish or gastropods. This is

447 in agreement with the phylogeographic studies of Joyce et al. (2005) and Schultheiß et al.

448 (2014) who considered Early to Middle Pleistocene age of Lake Palaeo-Makgadikgadi

449 evolutionary radiations, indicating palaeohydrology and hydromorphology differed

450 significantly from our observed MIS 5 setting.

451   In respect of pH, it can be inferred from the diatoms that the lake was always alkaline

452 (pH ~8). Whereas *C. meneghiniana*, *E. sorex*, *H. thermalis* and *R. gibberula* occur preferentially

453 in waters with the pH greater than 8 (Cholnoky 1968; Gasse 1986; Gasse et al. 1995; van Dam

454 et al. 1994), *M. elliptica* and *P. brevistriata* predominantly occur in circumneutral to low

455 alkaline waters (pH = 7-8; Cholnoky 1968; Gasse 1986; van Dam et al. 1994; Stachura-

456 Suchoples 2001; Fig. 4). In addition, *P. brevistriata*, *C. meneghiniana*, and *E. sorex* indicate

457 elevated trophic levels troughout the record (Cholnoky 1968; van Dam et al. 1994; Gasse et al.

458 1995; Krammer and Lange-Bertalot 2000; Stachura-Suchoples 2001; Kelly et al. 2005).

459   The $\delta^{18}O_{diatom}$ data reflects the oxygen isotope composition of lake water ($\delta^{18}O_{lake}$), and

460 the water temperature at the time of frustule formation (Leng and Barker 2006; Leng and

461 Henderson 2013). In turn, $\delta^{18}O_{lake}$ is controlled by the isotopic composition of precipitation

462 ($\delta^{18}O_{p}$) re-charging the lake and the balance of evaporation over precipitation on the lake. Open

463 lake systems that have permanent river inflow and outflow have short residence times, and as

464 a result $\delta^{18}O_{diatom}$ tends to reflect changes in $\delta^{18}O_{p}$. Whereas in closed lakes that have no

465 discernable outflow, $\delta^{18}O_{lake}$ is usually influenced by evaporation of surface waters, and as a

466 result $\delta^{18}O_{diatom}$ reflects the moisture balance (precipitation over evaporation) of the region

467 (Leng and Marshall 2004; Leng and Barker 2006; Leng and Henderson 2013).

468 There is scant information about the isotope composition of precipitation ($\delta^{18}O_p$) in

469 Botswana, and southern Africa in general, with much of our understanding of isotope dynamics

470 linked to changes in Late Pleistocene groundwater and speleothem $\delta^{18}O$ records (de Vries et al.

471 2000; Lee-Thorp et al. 2001; Holmgren et al. 2003; Kulongoski and Hilton 2004). The ^{18}O

472 enrichment of older groundwaters in Uitenhage, South Africa, have previously been interpreted

473 in terms of a change in moisture source, with a northeastward incursion of South Atlantic winter

474 precipitation, which displaces or mixes with monsoonal precipitation from the Indian Ocean in

475 south-western Africa (Stute and Talma 1998). By comparison, a more recent study from

476 Letlhakeng, southern Botswana, suggests there was no role for Atlantic-sourced moisture and

477 that the Indian Ocean has been the dominant moisture source over the southern Kalahari since

478 the Late Pleistocene through to the present day (Kulongoski and Hilton 2004). The influence

479 of the 'amount effect' on $\delta^{18}O_p$ has also been discounted, as modern $\delta^{18}O_p$ values for the region

480 range from 0 to –5‰, but the most depleted $\delta^{18}O_p$ values occur during months with the most

481 amount of rainfall (de Vries et al. 2000). As a result, Kulongoski et al. (2004) concluded that

482 Late Pleistocene groundwater $\delta^{18}O$ variability is caused by changes in atmosphere-$\delta^{18}O_p$

483 dynamics driven by changing sea surface temperatures.

484 A $\delta^{18}O$ speleothem record from Cold Air Cave in the Makapansgat Valley, northern South

485 Africa, was interpreted in terms of $\delta^{18}O_p$ variability caused by changes in the frequency of

486 intense convective storm events during the dry season that bring depleted $\delta^{18}O_p$ (Rozanski et

487 al. 1993), against a background of persistent mid-latitude rain during the wet season (Holmgren

488 et al. 2003). As a result, higher or more positive $\delta^{18}O_p$ values reflect generally warmer, wetter

489 conditions while lower values suggest cooler, drier conditions. This interpretation is supported

490   by a 100-year data set from the region, which demonstrates a positive correlation between

491   measured regional temperatures and speleothem $\delta^{18}O$ (Lee-Thorp et al. 2001). In addition, an

492   observed correlation between regional temperature and precipitation and speleothem colour,

493   layer thickness and $\delta^{18}O$ further supports the interpretation that lighter $\delta^{18}O_p$ is representative

494   of drier, colder conditions over southern Africa (Holmgren et al. 1999).

495   The $\delta^{18}O_{diatom}$ record from the BT unit spans approximately 1 ka sometime during MIS 5d-

496   b and shows decadal to bi-decadal variability. Based on the interpretative framework for

497   changes in $\delta^{18}O_p$ during the Late Pleistocene set out above, the shift in $\delta^{18}O_{diatom}$ from +30.5‰

498   at the base of the sediment unit to higher values of +34.2‰ at 11.5 cm would indicate

499   increasingly warmer and wetter conditions during this period (Fig. 4). The lower $\delta^{18}O_{diatom}$

500   values would be driven by the enhancement of a wet season over the Kalahari and an subsequent

501   increase in lake level. This observation is consistent with the increase in P/B ratio (Fig. 4),

502   suggesting an increase in planktonic habitats associated with greater lake levels. Moreover, on

503   top of an increasing lake level, the lake water would also be undergoing enhanced evaporation

504   because of the generally warmer conditions, and therefore lake waters would also become

505   further enriched in ^{18}O. Taken together, the shift to a dominant wet season and greater

506   evaporation would both drive $\delta^{18}O_{diatom}$ to the more positive values observed in our record (Fig.

507   4). However, it is difficult to tease out which would be the dominant mechanism, and the

508    $\delta^{18}O_{diatom}$ record is likely to reflect a combination of both.

509   After the initial increase there are a number of significant fluctuations in $\delta^{18}O_{diatom}$ from

510   ~+34 to +30.5‰ between 11.5 – 19.5 cm (Fig. 4), which broadly mirror changes in P/B, and

511   could reflect variability between warm-wet and cold-arid climate, as well as the subsequent

512   changes in evaporative concentration of Lake Palaeo-Makgadikgadi. Following this, the shift

513   to the lowest $\delta^{18}O_{diatom}$ values in our record occurs at 23.5 cm (Fig. 4), which we interpret as a

514   shift to colder and more arid conditions, as well as a lowering of lake level as indicated by the

515 P/B ratio from the diatom assemblages. The return to more positive $\delta^{18}O_{diatom}$ values after this

516 event (Fig. 4) could reflect a shift back to a warm, wet environment, but as the P/B ratios show,

517 lake levels remain low and so could reflect enhanced evaporation of lake water during this arid

518 stage in climate.

519 The relatively short duration of the mega-lake phase of approximately 1 ka under a

520 generally arid climate over large parts of southern Africa during MIS 5 (Scholz et al. 2007;

521 Urrego et al. 2015) suggests we may have captured a climate event at the scale of a Heinrich

522 event (Bond and Lotti 1995, Broecker 2002). Previous studies have modelled the impact of

523 Heinrich events on South Atlantic sea surface temperatures, which increase abruptly ("Atlantic

524 Heat Piracy Model", Ganopolski and Rahmstorf 2001; Seidov and Maslin 2001). The climatic

525 effect of northern hemisphere triggered Heinrich events on the southern hemisphere has also

526 been identified in Antarctica ice cores (Jouzel et al. 2007). The observation of Urrego et al.

527 (2015) that during climate transitions between warm and cold or cold and warm, humidity

528 during arid MIS 5 temporarily increased, supports the idea of a Heinrich event-like climate

529 period. Our record thus demonstrates the decadal to bi-decadal climate variability during such

530 an event.

531 Our data cannot contribute to the discussion whether the MIS 5 climate extremes

532 triggered large scale early human migration across and ultimatively out of Africa (Carto et al.

533 2009; Rito et al. 2013). The data, however, can contribute to the discussion why the Kalahari

534 hunter-gatherers, i.e. the Khoisan-speaking Bushmen groups, represent the genetically most

535 divergent population in the world (Tishkoff et al. 2007; Li et al. 2008; Henn et al. 2011). High

536 genetic variation means high adaptation potential (Charlesworth 2009). Semi-arid areas such as

537 the Kalahari are particularly vulnerable because small negative changes in precipitation amount

538 or in rainfall seasonality may trigger major changes in the environment and thus largely control

539 the habitability. Even under the assumption of large dating uncertainties, it is clear that

540 anatomically modern humans have lived in the Kalahari during MIS 5 and the climate extremes

541   likely triggered migration to environmentally more favourable regions. On the other hand it is

542   evident that Khoisan-speaking groups have adapted to arid climate, exhibiting traits which are

543   absent in other human groups such as the ability to store water and lipid metabolites in body

544   tissues (Schuster et al. 2010). Considering these adaptations in the context of archaeological

545   findings (Robbins et al. 2016), it can be assumed that Khoisan-speaking groups have lived

546   permanently in (semi-)arid environments since MIS 5, that is they probably never left the

547   Kalahari as other human groups did. The environmental history of the Kalahari since MIS 5

548   appears to be that of a highly dynamic and thus often fragmented ecosystem; habitat

549   fragmentation leading to human population fragmentation. Small populations however are

550   prone to genetic drift, which results in loss of genetic variation (Charlesworth 2009). Against

551   this background it can be suggested that the Khoisan-speaking groups have not been fragmented

552   into small populations but represented a relatively large human population all over the Kalahari.

553   This was possible only if these humans and the animals they hunted had access to potable water.

554   The here studied MIS 5 lake highstand in the MOZB of approximately 1 ka appears to

555   be a relatively short period, which however, can be compared with the tip of an iceberg. We do

556   not know how far the lake regressed after the highstand. We do not know how the seasonality

557   of MIS 5 rainfall was. We do not know which rivers were active during which period of

558   supposedly extra-arid MIS 5, except that we can assume from the geographical settings of

559   headwaters that Okavango, Orange and Zambezi rivers were likely perennial even during

560   megadroughts. These river systems however cannot have been the only sources of potable water

561   because otherwise the Khoisan-speaking population would have been fragmented, which

562   evidently was not the case. The idea that the Kalahari was even drier than present-day during

563   much of the last approximately 100 ka as was postulated for MIS 5 (Urrego et al. 2015) or for

564   the Last Glacial Maximum (LGM; Riedel et al. 2014) must be questioned. Gasse et al. (2008)

565   saw evidence for enhanced humidity over parts of south-western Africa during LGM. Hürkamp

566   et al. (2011) proposed winter rainfall in addition to summer rainfall over the southern Kalahari

567   during this period and Riedel et al. (2014) suggested that the Okwa River (Fig. 1) was fully

568   active during the LGM. It thus can be speculated that future studies of MIS 5 climate over the

569   Kalahari may exhibit the environment was more favourable for humans than supposed.

570

571   **Conclusions**

572

573   OSL ages suggest the identified mega-lake phase in the Kalahari occurred during a period of

574   MIS 5d-b. The climate over southern Africa during MIS 5 was considered to have been

575   (extremely) arid (Scholz et al. 2007; Urrego et al. 2015), although Urrego et al. (2015) identified

576   short excursions to more humid conditions during cold-warm and warm-cold transitions. One

577   of these humid periods triggered a highstand at Lake Palaeo-Makgadikgadi of about 935-940

578   m a.s.l. for approximately 1 ka, as is tentatively estimated here based on the potential

579   sedimentation rate of the studied section. This short-term hydrologically favorable phase is at

580   the scale of a North Atlantic-driven Heinrich event, and we speculate whether rapid increases

581   of southern Atlantic SSTs could have triggered significantly increased moisture supply over the

582   Kalahari and/or the Bié Plateau (Angola) where the (nowadays) active catchment of the

583   Okavango river system is located (Fig. 1).

584   The studied section is in close proximity to the palaeo-shore of the mega-lake and based

585   on the P/B ratio of diatom assemblages we infer shallow water conditions prevailed at the site.

586   The analysed diatom assemblages indicate an alkaline and oligohaline lake, although the

587   reconstructed salinity is not representative of the whole mega-lake because the studied section

588   is located about 100-150 km away from the two major inflow systems, the Okavango River in

589   the (north-)west and the Okwa River in the southwest of the lacustrine basins (Fig. 1). As we

590   could not infer which of the inflow systems was active during the highstand, a salinity gradient

591   from freshwater to oligohaline either existed off the Okavango or Okwa river mouths.

592   Considering the role Pleistocene Lake Palaeo-Makgadikgadi is likely to have played in

593 the phylogeography of freshwater fish (Joyce et al. 2005) or freshwater gastropods (Schultheiß

594 et al. 2014), we suggest the mega-lake phase in this study is too short a duration that is

595 dominated by oligohaline conditions, and therefore it was not a suitable trigger for evolutionary

596 radiations of freshwater taxa. The comparatively high temporal resolution of 1-2 decades of our

597 studied samples provides valuable insights of climate variability during a mega-lake phase.

598 Albeit significant changes in $\delta^{18}O_{diatom}$ values occurred (Fig. 4), the highstand is considered a

599 hydrologically stable period.

600   Although the studied mega-lake period was likely a short-term climate anomaly possibly

601 triggered by North-Atlantic iceberg discharges, it is challenging the view that MIS 5 was mostly

602 extremely dry. That the environment may have hydrologically been more favourable, is

603 supported by archaeological and genetic data suggesting permanent human occupation of the

604 Kalahari since MIS 5.

605

606 **Acknowledgements**

607

616

617 **References**

618

619   Balter M (2002) What made humans modern? Science 295(5558):1219-1225

620   Batisani N, Yarnal B (2010) Rainfall variability and trends in semi-arid Botswana: Implications

621   for climate change adaptation policy. Appl Geogr 30:483-489

622   Battarbee RW, Carvalho L, Jones VJ, Flower RJ, Cameron NG, Bennion H, Juggins S (2001)

623   Diatoms. In: Smol JP, Birks HJB, Last WM (eds) Tracking environmental change using

624   lake sediments, vol 3. Kluwer Academic Publishers, Dordrecht, pp 155-202

625   Bond GC, Lotti R (1995) Iceberg discharges into the North Atlantic on millennial time scales

626   during the last glaciation. Science 267:1005-1017

627   Bøtter-Jensen L (1997) Luminescence techniques: Instrumentation and methods. Radiat Meas

628   17:749-768

629   Broecker WS (2002) Massive iceberg discharges as triggers for global climate change. Nature

630   372:421-424

631   Burrough SL (2016) Late Quaternary environmental change and human occupation of the

632   southern African interior. In: Jones SC, Stewart BA (eds) Africa from MIS 6-2: Population

633   dynamics and palaeoenvironments – Vertebrate Paleobiology and Paleoanthropology

634   Series. Springer, Heidelberg, pp 161-174

635   Burrough SL, Thomas DSG (2009) Geomorphological contributions to palaeolimnology on the

636   African continent. Geomorphology 103:285-298

637   Burrough SL, Thomas DSG, Bailey RM (2009a) Mega-lake in the Kalahari: a late Pleistocene

638   record of the Palaeolake Makgadikgadi system. Quat Sci Rev 28:1392-1411

639   Burrough SL, Thomas DSG, Singarayer JS (2009b) Late Quaternary hydrological dynamics in

640   the Middle Kalahari: forcing and feedbacks. Earth-Sci Rev 96:313-326

641   Caljon AG, Cocquyt CZ (1992) Diatoms from surface sediments of the northern part of Lake

642   Tanganyika. Hydrobiologia 230:135-156

643   Carto SL, Weaver AJ, Hetherington R, Lam Y, Wiebe EC (2009) Out of Africa and into an ice

644   age: on the role of global climate change in the late Pleistocene migration of early modern

645   humans out of Africa. J Hum Evol 56:139-151

646   Chapligin B, Leng MJ, Webb E, Alexandre A, Dodd JP, Ijiri A, Lücke A, Shemesh A,

647   Abelmann A, Herzschuh H, Longstaffe FJ, Meyer H, Moschen R, Okazaki Y, Rees NH,

648   Sharp ZD, Sloane HJ, Sonzongi C, Swann JEA, Sylvestre F, Tyler JJ, Yam R (2011) Inter-

649   laboratory comparison of oxygen isotope compositions from biogenic silica. Geochim

650   Cosmochim Acta 75:7242-7256

651   Charlesworth B (2009) Effective population size and patterns of molecular evolution and

652   variation. Nat Rev Genet 10:195-205

653   Chase BM, Brewer S (2009) Last Glacial Maximum dune activity in the Kalahari desert of

654   southern Africa: observations and simulations. Quat Sci Rev 28:301-307

655   Chase BM, Meadows ME (2007) Late Quaternary dynamics of southern Africa´s winter rainfall

656   zone. Earth-Sci Rev 84:103-138

657   Chase BM, Scott L, Meadows ME, Gil-Romera G, Boom A, Carr AS, Reimer PJ, Truc L,

658   Valsecchi V, Quick LJ (2012) Rock hyrax middens: a palaeoenvironmental archive for

659   southern African drylands. Quat Sci Rev 56:107-125

660   Cholnoky BJ (1968) Die Ökologie der Diatomeen in Binnengewässern (Ecology of diatoms in

661   inland waters). Cramer J, Lehre, Germany

662   Cohen AS, Stone JR, Beuning KRM, Park LE, Reinthal PN, Dettman D, Scholz CA, Johnson

663   TC, King JW, Talbot MR, Brown ET, Ivory SJ (2007) Ecological consequences of early

664   Late Pleistocene megadroughts in tropical Africa. PNAS 104(42):16422-16427

665   Cooke HJ (1979) The origin of the Makgadikgadi Pans. Botsw Notes Rec 11:37-42

666   Cooke HJ (1980) Landform evolution in the context of climatic change and neo-tectonism in

667   the Middle Kalahari of north-central Botswana. Trans Inst Br Geogr 5:80-99

668   Cooke HJ, Verstappen HT (1984) The landforms of the western Makgadikgadi basin in northern

669   Botswana, with consideration of the chronology of the evolution of Lake Palaeo-

670   Makgadikgadi. Z Geomorphol 28:1–19

671   Cordier S, Harmand D, Lauer T, Voinchet P, Bahain JJ, Frechen M (2012) Geochronological

672   reconstruction of the Pleistocene evolution of the Sarre valley (France and Germany) using

673   OSL and ESR dating techniques. Geomorphology 165-166:91-106

674   de Vries JJ, Selaolo ET, Beekman HE (2000) Groundwater recharge in the Kalahari, with

675   reference to paleo-hydrologic conditions. J Hydrol 238:110–123

676   Ebert JI, Hitchcock, RK (1978) Ancient lake Makgadikgadi, Botswana: mapping measurement

677   and palaeoclimate significance. Palaeoecol Afr 10/11:47-56

678   Eckardt FD, Bryant RG, McCulloch G, Spiro B, Wood WW (2008) The hydrochemistry of a

679   semi-arid pan basin case study: Sua Pan, Makgadikgadi, Botswana. Appl Geochem

680   23:1563-1580

681   Filippov A, Riedel F (2009) The late Holocene mollusc fauna of the Aral Sea and its

682   biogeographical and ecological interpretation. Limnologica 39:67-85

683   Fornace KL, Hughen KA, Shanahan TM, Fritz SC, Baker PA, Sylvia SP (2014) A 60,000-year

684   record of hydrologic variability in the Central Andes from the hydrogen isotopic

685   composition of leaf waxes in Lake Titicaca sediments. Earth Planet Sci Lett 408:263-271

686   Gabriel KR (2002) Goodness of fit of biplots and correspondence analysis. Biometrika 89:423-

687   436

688   Ganopolski A, Rahmstorf S (2001) Rapid changes of glacial climate simulated in a coupled

689   climate model. Nature 409:153-158

690   Gasse F (1986) East African diatoms – Taxonomy, ecological distribution. Bibl Diatomol 11:1–

691   201

692 Gasse F, Juggins S, Ben Khelifa L (1995) Diatom-based transfer functions for inferring past

693   hydrochemical characteristics of African lakes. Palaeogeogr, Palaeoclimatol, Palaeoecol

694   117:31-54

695 Gasse F, Chalié F, Vincens A, Williams MAJ, Williamson D (2008) Climatic patterns in

696   equatorial and southern Africa from 30,000 to 10,000 years ago reconstructed from

697   terrestrial and near-shore proxy data. Quat Sci Rev 27:2316-2340

698 Genner MJ, Seehausen O, Lunt DH, Joyce DA, Shaw PW, Carvalho GR, Turner GF (2007)

699   Age of cichlids – new dates for ancient fish radiations. Mol Biol Evol 24:1269-1282

700 Geyh MA, Heine K (2014) Several distinct wet periods since 420 ka in the Namib Desert

701   inferred from U-series dates of speleothems. Quat Res 81(2):381-391

702 Grey DRC, Cooke HJ (1977) Some problems in the Quaternary evolution of the landforms of

703   northern Botswana. Catena 4:123-133

704 Grimm EC (1991-2011) Tilia®Version 1.7.16 [Computer Software] Illinois State Museum,

705   Research and Collection Center, Springfield

706 Grove AT (1969) Landforms and climatic change in the Kalahari and Ngamiland. Geogr J

707   135:191-212

708 Gumbricht T, McCarthy TS, Merry CL (2001) The topography of the Okavango Delta,

709   Botswana, and its tectonic and sedimentological implications. S Afr J Sci 104:243-264

710 Haddon IG, McCarthy TS (2005) The Mesozoic-Cenozoic interior sag basins of central Africa

711   – The Late-Cretaceous-Cenozoic Kalahari and Okavango basins. J Afr Earth Sci 43:316-

712   333

713 Hecky RE, Kilham P (1973) Diatoms in alkaline, saline lakes: Ecology and geochemical

714   implications. Limnol Oceanogr 18:53-71

715 Heine K (1981) Aride und pluviale Bedingungen während der letzten Kaltzeit in der Südwest-

716   Kalahari (südliches Afrika)(Arid and pluvial conditions during the last glacial in the

717   southwest Kalahari (southern Africa)). Z Geomorphol NF, Suppl 38:1-37

718 Heine K (1982) The main stages of the Late Quaternary evolution of the Kalahari region,
719   southern Africa. Palaeoecol Afr 15:53-76

720 Heine K (1987) Zum Alter jungquartärer Seespiegelschwankungen in der Mittleren Kalahari,
721   südliches Afrika (On the age of late Quaternary lake level fluctuations in the Middle
722   Kalahari, southern Africa). Palaeoecol Afr 18:73-101

723 Heine K (1988) Southern African palaeoclimates 35-25 ka ago: a preliminary summary.
724   Palaeoecol Afr 19:305-315

725 Henn BM, Gignoux CR, Jobin M, Granka JM, Macpherson JM, Kidd JM, Rodríguez-Botigué
726   L, Ramachandran S, Hon L, Brisbin A, Lin AA, Underhill PA, Comas D, Kidd KK,
727   Norman PJ, Parham P, Bustamante CD, Mountain JL, Feldman MW (2011) Hunter-
728   gatherer genomic diversity suggests a southern African origin for modern humans. PNAS
729   108(13):5154-5162

730 Henshilwood CS, d´Errico F, Yates R, Jacobs Z, Tribolo C, Duller GAT, Mercier N, Sealy JC,
731   Valladas H, Watts I, Wintle AG (2002) Emergence of modern human behavior: Middle
732   Stone Age engravings from South Africa. Science 295(5558):1278-1280

733 Holmgren K, Lee-Thorp, JA, Cooper GRJ, Lundblad K, Partridge TC, Scott L, Sithaldeen R,
734   Talma AS, Tyson PD (2003) Persistent millennial-scale climatic variability over the past
735   25,000 years in Southern Africa. Quat Sci Rev 22:2311-2326

736 Holmgren K, Karlén W, Lauritzen SE, Lee-Thorp JA, Partridge TC, Piketh S, Repinski P,
737   Stevenson C, Svenered O, Tyson PD (1999) A 3000-year high-resolution stalagmite based
738   record of palaeoclimate for northeastern South Africa. Holocene 9:295-309

739 Hürkamp K, Völkel J, Heine K, Bens O, Leopold M, Winkelbauer J (2011) Late Quaternary
740   environmental changes from aeolian and fluvial geoarchives in the south-western Kalahari,
741   South Africa: implications for past African climate dynamics. S Afr J Geol 114:459-474

742 Ingman M, Kaessmann H, Pääbo S, Gyllensten U (2000) Mitochondrial genome variation and
743   the orgin of modern humans. Nature 408:708-713

744 Jacobs Z, Roberts RG (2009) Catalysts for Stone Age innovations. Commun Integr Biol
745   2(2):191-193

746 Jollifer IT (1986) Principal Components Analysis. Springer-Verlag, New York

747 Jouzel J, Masson-Delmotte V, Cattani O, Dreyfus G, Falourd S, Hoffmann G, Minster B, Nouet
748   J, Barnola JM, Chappellaz J, Fischer H, Gallet JC, Johnsen S, Leuenberger M, Loulergue
749   L, Luethi D, Oerter H, Parrenin F, Raisbeck G, Raynaud D, Schilt A, Schwander J, Selmo
750   E, Souchez R, Spahni R, Stauffer B, Steffensen JP, Stenni B, Stocker TF, Tison JL, Werner
751   M, Wolff W (2007) Orbital and millennial Antarctic climate variability over the past
752   800,000 Years. Science 317:793-796

753 Joyce DA, Lunt DH, Bills R, Turner GF, Katongo C, Duftner N, Sturmbauer C, Seehausen O
754   (2005) An extant cichlid fish radiation emerged in an extinct Pleistocene lake. Nature
755   435:90-95

756 Kelly MG, Bennion H, Cox EJ, Goldsmith B, Jamieson J, Juggins S, Mann DG, Telford RJ
757   (2005) Common freshwater diatoms of Britain and Ireland – an interactive key.
758   Environment Agency, Bristol: http://craticula.ncl.ac.uk/ EADiatomKey/html/taxa.html

759 Kinabo BD, Atekwana EA, Hogan JP, Modisi MP, Wheaton DD, Kampunzu AB (2007) Early
760   structural development of the Okavango rift zone, NW Botswana. J Afr Earth Sci 48:125-
761   136

762 Kostrova SS, Meyer H, Tarasov PE, Bezrukova EV, Chapligin B, Kossler A, Pavlova LA,
763   Kuzmin MI (2016) Oxygen isotope composition of diatoms from sediments of Lake
764   Kotokel. Russ Geol Geophys 57:1239-1247

765 Krammer K (2002) *Cymbella*. In: Lange-Bertalot H (ed) Diatoms of Europe, vol 3. ARG
766   Gantner Verlag KG, Ruggell

767 Krammer K, Lange-Bertalot H (1997) Bacillariophyceae. Part 1, Naviculaceae. In: Ettl H,
768   Gerloff J, Heynig H, Mollenhauer D (eds) Süßwasserflora von Mitteleuropa 2/1
769   (Freshwater flora from Central Europe). Spektrum Akademischer Verlag, Heidelberg

770   Krammer K, Lange-Bertalot H (1999) Bacillariophyceae. Part 2, Bacillariaceae, Epithemiaceae, Surirellaceae. In: Ettl H, Gerloff J, Heynig H, Mollenhauer D (eds) Süßwasserflora von Mitteleuropa 2/2 (Freshwater flora from Central Europe). Spektrum Akademischer Verlag, Heidelberg, Berlin

774   Krammer K, Lange-Bertalot H (2000) Bacillariophyceae. Part 3, Centrales, Fragilariaceae, Eunotiaceae. In: Ettl H, Gerloff J, Heynig H, Mollenhauer D (eds) Süßwasserflora von Mitteleuropa 2/3 (Freshwater flora from Central Europe). Spektrum Akademischer Verlag, Heidelberg, Berlin

778   Krammer K, Lange-Bertalot H (2004) Bacillariophyceae. Part 4, Achnanthaceae, Kritische Ergänzungen zu *Achnanthes* s.i., *Navicula* s.str., *Gomphonema*. In: Ettl H, Gärtner G, Heynig H, Mollenhauer D (eds) Süßwasserflora von Mitteleuropa 2/4 (Freshwater flora from Central Europe). Spektrum Akademischer Verlag, Heidelberg, Berlin

782   Kulongoski JT, Hilton DR (2004) Climate variability in the Botswana Kalahari from the late Pleistocene to the present day. Geophys Res Lett 31:doi:10.1029/2003GL019238

784   Kusber W-H, Cocquyt CZ (2012) *Craticula elkab* (O. Müller ex O. Müller) Lange-Bertalot, Kusber & Cocquyt, comb. nov. - Typification and observations based on African sediment core material. Diatom Res 22:117-126

787   Lee-Thorp JA, Holmgren K, Lauritzen SE, Linge H, Moberg A, Partridge TC, Stevenson C, Tyson PD (2001) Rapid climate shifts in the southern African interior throughout the mid to late Holocene. Geophys Res Lett 28:4507-4510

790   Leipe C, Demske D, Tarasov PE, Wünnemann B, Riedel F, HIMPAC project members (2014) Potential of pollen and non-pollen palynomorph records from Tso Moriri (Trans-Himalaya, NW India) for reconstructing Holocene limnology and human-environmental interactions. Quat Int 348:113-129

794   Leng MJ, Barker PA (2006) A review of the oxygen isotope composition of lacustrine diatom silica for palaeoclimate reconstruction. Earth-Sci Rev 75:5-27

796   Leng MJ, Henderson ACG (2013) Recent advances in isotopes as palaeolimnological proxies.

797   J Paleolimnol 49:481-496

798   Leng MJ, Marshall JD (2004) Palaeoclimate interpretation of stable isotope data from lake

799   sediment archives. Quat Sci Rev 23:811-831

800   Leng MJ, Sloane HJ (2008) Combined oxygen and silicon isotope analysis of biogenic silica. J

801   Quaternary Sci 23:313-319

802   Levkov Z (2009) *Amphora* sensu lato. In: Lange-Bertalot H (ed) Diatoms of Europe, vol 5,

803   ARG Gantner KG, Ruggell

804   Li JZ, Absher DM, Tang H, Southwick AM, Casto AM, Ramachandran S, Cann HM, Barsh

805   GS, Feldman M, Cavalli-Sforza LL, Myers RM (2008) Worldwide human relationships

806   inferred from genome-wide patterns of variation. Science 319(5866):1100-1104

807   Lotter AF, Birks HJB (1993) The impact of the Laacher See tephra on terrestrial and aquatic

808   ecosystems in the Black Forest, southern Germany. J Quaternary Sci 8:263-276

809   Mackay AW, Davidson T, Wolski P, Woodward S, Mazebedi R, Masamba WRL, Todd M

810   (2012) Diatom sensitivity to hydrological and nutrient variability in a subtropical, flood-

811   pulse wetland. Ecohydrology 5:491-502

812   Mallick DIJ, Habgood F, Skinner AC (1981) A geological interpretation of Landsat imagery

813   and airphotography of Botswana. Overseas Geol Mineral Resour 56:1-35

814   Marean CW, Bar-Matthews M, Bernatchez J, Fisher E, Goldberg P, Herries AIR, Jacobs Z,

815   Jerardino A, Karkanas P, Minichillo T, Nilssen PJ, Thompson E, Watts I, Williams HM

816   (2007) Early human use of marine resources and pigment in South Africa during the Middle

817   Pleistocene. Nature 449:905-909

818   Mischke S, Wünnemann B (2006) The Holocene salinity history of Bosten Lake (Xinjiang,

819   China) inferred from ostracod species assemblages and shell chemistry: Possible

820   palaeoclimatic implications. Quat Int 154-155:100-112

821   Mitrofanova EY, Sutchenkova OS, Lovtskaya OV (2016) Lake Teletskoye (Altai, Russia):

822   reconstruction of the environment and prediction for its changes according to the

823   composition and quantity of diatoms in the bottom sediments. Russ Geol Geophys

824   57:1321-1333

825 Moore AE, Cotterill FPD, Eckardt FD(2012) The evolution and ages of Makgadikgadi palaeo-

826   lakes – consilient evidence from Kalahari drainage evolution, Botswana. S Afr J Geol

827   115:385-413

828 Morley DW, Leng MJ, Mackay AW, Sloane HJ, Rioual P, Battarbee RW (2004) Cleaning of

829   lake sediments for diatom oxygen isotope analysis. J Paleolimnol 31:391-401

830 Murray A, Wintle A (2000) Luminescence dating of quartz using an improved single-aliquot

831   regenerative-dose protocol. Radiat Meas 32:57-73

832 Nugent C (1990) The Zambezi River – tectonism, climatic change and drainage evolution.

833   Palaeogeogr Palaeoclimat Palaeoecol 78:55-69

834 Passarge S (1904) Die Kalahari (The Kalahari). Dietrich Riemer, Berlin

835 Patrick R (1977) The ecology of freshwater diatoms – diatom communities. In: Werner D (ed)

836   The Biology of Diatoms. University of California Press, Berkeley, Los Angeles, pp 284-

837   332

838 Peel MC, Finlayson BL, McMahon TA (2007) Updated world map of the Köppen-Geiger

839   climate classification. HESSD 4:439-473

840 Podgorski JE, Green AG, Kgotlhang L, Kinzelbach WKH, Kalscheuer T, Auken E, Ngwisanyi

841   T (2013) Paleo-megalake and paleo-megafan in southern Africa. Geology 41:1155-1158

842 Prescott JR, Hutton JT (1994) Cosmic Ray Contributions to Dose Rates for Luminescence and

843   ESR Dating: Large Depths and Long-Term Time Variations. Radiat Meas 23:497-500

844 Riedel F, Erhardt S, Chauke C, Kossler A, Shemang E, Tarasov P (2012) Evidence for a

845   permanent lake in Sua Pan (Kalahari, Botswana) during the early centuries of the last

846   millenium indicated by distribution of Baobab trees (*Adansonia digitata*) on "Kubu Island".

847   Quat Int 253:67-73

848   Riedel F, Henderson ACG, Heußner KU, Kaufmann G, Kossler A, Leipe C, Shemang E, Taft

849   L (2014) Dynamics of a Kalahari long-lived mega-lake system – hydromorphological and

850   limnological changes in the Makgadikgadi Basin (Botswana) during the terminal 50 ka.

851   Hydrobiologia 739:25-53

852   Ringrose S, Huntsman-Mapila P, Kampunzu AB, Downey WS, Coetzee SH, Vink B, Matheson

853   W, Vanderpost C (2005) Sedimentological and geochemical evidence for palaeo-

854   environmental change in the Makgadikgadi subbasin, in relation to the MOZ rift

855   depression, Botswana. Palaeogeogr Palaeoclimatol Palaeoecol 217:265-287

856   Rito T, Richards MB, Fernandes V, Alshamali F, Cerny V, Pereira L, Soares P (2013) The first

857   modern human dispersal across Africa. PLOS ONE 8(11)e80031

858   Robbins LH, Brook GA, Murphy ML, Ivester AH, Campbell AC (2016) The Kalahari during

859   MIS 6-2 (190-12 ka): Archaeology, paleoenvironment, and population dynamics. In: Jones

860   SC, Stewart BA (eds) Africa from MIS 6-2: Population dynamics and palaeoenvironments

861   – Vertebrate Paleobiology and Paleoanthropology Series. Springer, Heidelberg, pp 175-

862   193

863   Rozanski K, Araguas-Araguas L, Gonfiantini R (1993) Isotopic patterns in modern global

864   precipitation. In: Climate change in continental isotopic records. Swart PK, Lohman KC,

865   McKenzie J, Savin S (eds), Geophysical Monograph 78:1-36

866   Schlungbaum G, Baudler H (2001) Die Vielfalt innerer Küstengewässer an der südlichen

867   Ostsee - eine Übersicht von der Flensburger Förde bis zum Kurischen Haff, Teil 1

868   Entwicklungsgeschichte, Morphologie, Hydrologie und Hydrographie (The diversity of

869   interior coastal waters at the southern Baltic Sea – an overview from the Flensburg Fjord

870   to the Curonian Lagoon, part 1 history of development, morphology, hydrology and

871   hydrography). Rostock Meeresbiolog Beitr 8:5-61

872   Scholz CA, Johnson TC, Cohen AS, King JW, Peck JA, Overpeck JT, Talbot MR, Brown ET,

873   Kalindekafe E, Amoako PYO, Lyons RP, Shanahan TM, Castañeda IS, Heil CW, Forman

874   SL, McHargue LR, Beuning KR, Gomez J, Pierson J (2007) East African megadroughts

875   between 135 and 75 thousand years ago and bearing on early-modern human origins. PNAS

876   104(42):16416-16421

877 Schultheiß R, Van Bocxlaer B, Riedel F, von Rintelen T, Albrecht C (2014) Disjunct

878   distributions of freshwater snails testify to a central role of the Congo system in shaping

879   biogeographical patterns in Africa. BMC Evol Biol 14:42

880 Schuster SC, Miller W, Ratan A, Tomsho LP, Giardine B, Kasson LR, Harris RS, Petersen DC,

881   Zhao FQ, Qi J, Alkan C, Kidd JM, Sun YZ, Drautz DI, Bouffard P, Muzny DM, Reid JG,

882   Nazareth LV, Wang QY, Burhans R, Riemer C, Wittekindt NE, Moorjani P, Tindall EA,

883   Danko CG, Siang Teo W, Buboltz AM, Zhang ZH, Ma QY, Oosthuysen A, Steenkamp

884   AW, Oosthuisen H, Venter P, Gajewski J, Zhang Y, Franklin Pugh B, Makova KD,

885   Nekrutenko A, Mardis ER, Patterson N, Pringle TH, Chiaromonte F, Mullikin JC, Eichler

886   EE, Hardison RC, Gibbs RA, Harkins TT, Hayes VM (2010) Complete Khoisan and Bantu

887   genomes from southern Africa. Nature 463:943-947

888 Seidov D, Maslin M (2001) Atlantic Ocean heat piracy and the bipolar climate see-saw during

889   Heinrich and Dansgaard-Oeschger events. J Quaternary Sci 16:321-328

890 Shaw PA, Stokes S, Thomas DSG, Davies FBM, Holmgren K (1997) Palaeoecology and age

891   of a Quaternary high lake level in the Makgadikgadi Basin of the Middle Kalahari,

892   Botswana. S Afr J Sci 93:273-276

893 Shemang EM, Molwalefhe LN (2011) Geomorphic landforms and tectonism along the eastern

894   margin of the Okavango Rift Zone, north western Botswana as deduced from geophysical

895   data in the area. In: Sharkov EV (ed) New frontiers in tectonic research – General problems,

896   sedimentary basins and island arcs. InTech, Rijeka, pp 169-182

897 Shi N, Schneider R, Beug HJ, Dupont LM (2001) Southeast trade wind variations during the

898   last 135 kyr: evidence from pollen spectra in eastern South Atlantic sediments. EPSL

899   187:311-321

900   Stachura-Suchoples K (2001) Bioindicative values of dominant diatom species from the Gulf

901   of Gdansk, Southern Baltic Sea, Poland. In: Jahn R, Kociolek JP, Witkowski A, Compère

902   P (eds) Lange-Bertalot Festschrift. ARG Gantner KG, Ruggell, pp 477-490

903   Stokes S, Thomas DSG, Washington R (1997) Multiple episodes of aridity in southern Africa

904   since the last interglacial period. Nature 388:154-158

905   Street FA, Grove AT (1976) Environmental and climatic implications of late Quaternary lake-

906   level fluctuations in Africa. Nature 261:385-390

907   Stute M, Talma AS (1998) Glacial temperature and moisture transport regimes reconstructed

908   from noble gases and $\delta^{18}O$, Stampriet aquifer, Namibia. In: Isotope techniques in the study

909   of environmental change. IAEA, Vienna, pp 307-318

910   Stuut JBW, Prins MA, Schneider RR, Weltje GJ, Jansen JHF, Postma G (2002) A 300-kyr

911   record of aridity and wind strength in southwestern Africa: inferences from grain-size

912   distributions of sediments on Walvis Ridge, SE Atlantic. Mar Geol 180:221-233

913   ter Braak CJF, Šmilauer P (2002) CANOCO Reference Manual and User's Guide to CANOCO

914   for Windows: Software for Canonical Community Ordination Version 4.5. Microcomputer

915   Power, Ithaca, New York

916   Thomas DSG, Shaw PA (1991) The Kalahari environment, Cambridge University Press,

917   Cambridge

918   Tishkoff SA, Gonder MK, Henn BM, Mortensen H, Knight A, Gignoux C, Fernandopulle N,

919   Lema G, Nyambo TB, Ramakrishnan U, Reed FA, Mountain JL (2007) History of click-

920   speaking populations of Africa inferred from mtDNA and Y chromosome genetic variation.

921   Mol Biol Evol 24(10):2180-2195

922   Urrego DH, Sánchez Goñi MF, Daniau AL, Lechevrel S, Hanquiez V (2015) Increased aridity

923   in southwestern Africa during the warmest periods of the last interglacial. Clim Past

924   11:1417-1431

925   van Dam H, Mertens A, Sinkeldam J (1994) A coded checklist and ecological indicator values

926   of freshwater diatoms from the Netherlands. Neth J Aquat Ecol 28:117–133

927   van Zinderen Bakker EM (1976) The evolution of Late-Quaternary palaeoclimates of southern

928   Africa. Palaeoecol Afr 9:160-202

929

ESM 2: Ecological information of the identified taxa with references

Species	b/p	salinity	pH	trophic level
R. gibba	b	freshwater[1]	indifferent (7 - 9)[1,2,3,4]	oligo- to eutraphentic[1,3,5]
S. engleri	b	freshwater[3]	optimum: 7.6 - 8[1]	
N. gracilis	b	freshwater[2]	widely indifferent 5.5-6[1]; 7-8[3]	oligo-[6] to mesotr.[2]; nitrogen heterotraphentic[1]
C. cf. lancettulif.	b	freshwater[7]		
F. rhomboides	b	freshwater[3]	acidophilous, 5.7 - 5.8[1]	oligotraphentic[2]
N. radiosa	b	freshwater[8]	6.5 - 7[1]	meso- to eutraphentic[2]
N. scutelloides	b	freshwater[9]	8 - 8.5[1,3,4]	eutraphentic[2]
P. esox	b	freshwater[10]	< 7[1,2]	mesotraphentic[2]
P. microstauron	b	freshwater[3]	6.5[3] - 7[1]	eutraphentic[2]
E. cf. diodon	b	freshwater[2]	5.3 - 5.4[1]	oligotraphentic[2]
A. exigua	b	freshwater[1]	8 - 9[1,4]	eutraphentic[11]
A. ambigua	p	freshwater[2]	slightly > 7[4]	eutraphentic[2]
G. angustatum	b	mostly freshwater[1]	7.5 - 8[1,3]	oligotraphentic[2]
G. cf. clavatum	b	mostly freshwater[12]	> 8[4]	oligotraphentic[2]
H. amphioxys	b	fresh water, tolerates oligohaline[1]	> 7, widely indifferent[1]	eurytraphentic[2]; nitrogen heterotraphentic[1,13,14]
A. copulata	b	freshwater to oligohaline[2]	8 - 9[2]	eutraphentic[2,15]
F. cf. capucina	p	freshwater to oligohaline[2]	7.4 - 7.8[1]	meso- to eutraphentic[2,15]
H. thermalis	b	freshwater to oligohaline[3]	8 - 9[3]	
H. veneta	b	freshwater to oligohaline[1]	8 - 8.5[1]	eutraphentic[1,2]
C. cf. elkab	b	freshwater to oligohaline[3]	8[1] - 9.4[4]	
M. martyi	b	freshwater[15] to oligohaline[5]	~ 8[1,4]	eu- to mesotraphentic[2]
S. construens	b	freshwater to oligohaline[15]	7.8[1] - 8.4[4]	eutraphentic[15]
D. stelligera	p	freshwater to oligohaline[1]	6.8 - 8.5[1,3,4]	eurytraphentic[1]
S. phoenicenteron	b	freshwater to oligohaline[2]	6.8 - 7[1,4]	eutraphentic[2]
P. gastrum	b	oligohaline, tolerates freshwater[5,9]	~ 8[1]	eutraphentic[2]
E. sorex	b	oligohaline[1,12,16,17]	> 8[2]; 8.3 - 8.5[1]	eutraphentic[1,2,12]
D. kuetzingii	b	oligohaline[2]	8 - 9[3]	mesotraphentic[2]
C. cymbiformis	b	oligohaline[2]	7.5 - 8[1,3]	oligotraphentic[2]
S. pupula	b	oligo- to mesohaline[1]	indifferent[3]	eurytraphentic[2]
C. meneghiniana	p	oligo- to mesohaline[1]	8 - 8.5[1,4]	eutraphentic[18]
A. sphaerophora	b	mesohaline to marine[8,15]	8 - 8.5[1]; tolerates pH ≥ 9[3]	eutraphentic[2]
C. clypeus	b	mesohaline to marine[16,19]	7 - 8[12]	eutraphentic[2]
R. gibberula	b	freshwater[9] to mesohaline[2]	widely indifferent; > 8 - 10[1,3]	oligo- to eutraphentic[1,20]
C. placentula	b	freshwater[1] to mesohaline[12]	8[4]	eutraphentic[2]
P. brevistriata	b	freshwater to mesohaline[2,15]	7.5 - 7.8[1,4]	eutraphentic[15,18]
T. cf. hungarica	b	mesohaline[2]; tolerates freshwater[12]	~ 8.5[1,2,3]	eutraphentic[2]
C. pusilla	b	mesohaline, tolerates freshwater[21]	7 - 8[3,4]	
N. cf. frustulum	b	mesohaline[1]; euryhaline[22]	8.7 - 10[1,4]	eutraphentic[2,12,23];nitrogen heterotr.c[1,14]
M. elliptica	b	mesohaline[1,24]; euryhaline[22]	7 - 8[1,2,3]	
C. solea	b	euryhaline[22]	slightly > 8[1]	eutraphentic[2]
S. ovalis	b	euryhaline[1,2]	~8[1,4]	eutraphentic[2]
D. stelligeroides	p			oligo- to mesotraphentic[25]
C. cucumis	b		7.5 - 8[1]	
E. volkii	b			
A. frickei	b			

[1]Cholnoky 1968; [2]van Dam et al. 1994; [3]Gasse 1986; [4]Gasse et al. 1995; [5]Hustedt 1957; [6]Cholnoky 1966b; [7]Guiry and Guiry 2012; [8]Krammer and Lange-Bertalot 1997; [9]Patrick and Reimer 1966; [10]Andrews 1966; [11]Krammer and Lange-Bertalot 2004; [12]Kelly et al. 2005; [13]Cocquyt 1998; [14]Round et al. 1990; [15]Stachura-Suchoples 2001; [16]Krammer and Lange-Bertalot 1999; [17]Patrick 1977; [18]Krammer and Lange-Bertalot 2000; [19]Poulíčková and Jahn 2007; [20]Patrick and Reimer 1975; [21]Cholnoky 1960; [22]Caljon and Cocquyt 1992; [23]Cholnoky 1966a; [24]Müller 1904; [25]Houk et al. 2010

References ESM 2

Andrews GW (1966) Late Pleistocene diatoms from the Trempealeau Valley, Wisconsin. Geol Surv Prof Paper 523:1-27

Caljon AG, Cocquyt CZ (1992) Diatoms from surface sediments of the northern part of Lake Tanganyika. Hydrobiologia 230:135-156

Cholnoky BJ (1960) Beiträge zur Kenntnis der Diatomeenflora von Natal, Südafrika (Contributions to the knowledge of the diatom flora of Natal, South Africa). Nova Hedwigia 2:1-128

Cholnoky BJ (1966a) Die Diatomeen aus dem Unterlaufe des Okawango-Flusses (Diatoms of the lower section of the Okavango). Beih Nova Hedwigia 21 (Diatomaceae I): 1-120

Cholnoky BJ (1966b) Diatomeenassoziationen aus einigen Quellen in Südwest-Afrika und Bechuanaland (Diatom assemblages from several springs in Southwest Africa and Bechuanaland). Beih Nova Hedwigia 21 (Diatomaceae I): 161-250

Cholnoky BJ (1968) Die Ökologie der Diatomeen in Binnengewässern (Ecology of diatoms in fresh waters). Cramer J, Lehre, Germany

Cocquyt CZ (1998) Diatoms from the northern basin of Lake Tanganyika. Bibl Diatomol 39:1-275

Guiry MD, Guiry GM (2012) AlgaeBase. World-wide electronic publication, National University of Ireland. http://www.algaebase.org, Galway

Gasse F (1986) East African diatoms – Taxonomy, ecological distribution. Bibl Diatomol 11:1–201

Gasse F, Juggins S, Ben Khelifa L (1995) Diatom-based transfer functions for inferring past hydrochemical characteristics of African lakes. Palaeogeogr, Palaeoclimatol, Palaeoecol 117:31-54

Houk V, Klee R, Tanaka H, Poulíčková A (2010) Atlas of freshwater diatoms with a brief key and descriptions: *Stephanodiscaceae* A, *Cyclotella*, *Tertiarius*, *Discostella*, Part III. Fottea 10(supplement):1-498

Hustedt F (1957) Die Diatomeenflora des Flusssystems der Weser im Gebiet der Hansestadt Bremen (Diatom flora of the Weser River streams in the region of Hansestadt Bremen). Abh Natwiss Ver Brem 34 (3):18-140

Kelly MG, Bennion H, Cox EJ, Goldsmith B, Jamieson J, Juggins S, Mann DG, Telford RJ (2005) Common freshwater diatoms of Britain and Ireland – an interactive key. Environment Agency, Bristol: http://craticula.ncl.ac.uk/ EADiatomKey/html/taxa.html

Krammer K, Lange-Bertalot H (1997) Bacillariophyceae. Part 1, Naviculaceae. In: Ettl H, Gerloff J, Heynig H, Mollenhauer D (eds) Süßwasserflora von Mitteleuropa 2/1 (Freshwater flora from Central Europe). Spektrum Akademischer Verlag, Heidelberg

Krammer K, Lange-Bertalot H (1999) Bacillariophyceae. Part 2, Bacillariaceae, Epithemiaceae, Surirellaceae. In: Ettl H, Gerloff J, Heynig H, Mollenhauer D (eds) Süßwasserflora von Mitteleuropa 2/2 (Freshwater flora from Central Europe). Spektrum Akademischer Verlag, Heidelberg, Berlin

Krammer K, Lange-Bertalot H (2000) Bacillariophyceae. Part 3, Centrales, Fragilariaceae, Eunotiaceae. In: Ettl H, Gerloff J, Heynig H, Mollenhauer D (eds) Süßwasserflora von Mitteleuropa 2/3 (Freshwater flora from Central Europe). Spektrum Akademischer Verlag, Heidelberg, Berlin

Krammer K, Lange-Bertalot H (2004) Bacillariophyceae. Part 4, Achnanthaceae, Kritische Ergänzungen zu *Achnanthes* s.i., *Navicula* s.str., *Gomphonema*. In: Ettl H, Gärtner G, Heynig H, Mollenhauer D (eds) Süßwasserflora von Mitteleuropa 2/4 (Freshwater flora from Central Europe). Spektrum Akademischer Verlag, Heidelberg, Berlin, pp 469

Müller O (1904) Bacillariaceen aus dem Nyassalande und einigen benachbarten Gebieten (Bacillariaceae from Niassa Province and adjacent regions) part 2, Sonderabdruck aus Engler's Botanischen Jahrb 34(2):256-301

Patrick R (1977) The ecology of freshwater diatoms – diatom communities. In: Werner D (ed) The Biology of Diatoms. University of California Press, Berkeley, Los Angeles, pp 284-332

Patrick R, Reimer CW (1966) The diatoms of the United States exclusive Alaska and Hawaii. Vol 1, Fragilariaceae, Eunotiaceae, Achnanthaceae, Naviculaceae. Academy of Natural Sciences of Philadelphia

Patrick R, Reimer CW (1975) The diatoms of the United States exclusive of Alaska and Hawaii. Vol 2.1, Entomoneidaceae, Cymbellaceae, Gomphonemaceae, Epithemiaceae. Academy of Natural Sciences of Philadelphia

Poulíčková A, Jahn R (2007) *Campylodiscus clypeus* (Ehrenberg) Ehrenberg ex Kützing – typification, morphology and distribution. Diatom Res 22:135-146

Round FE, Crawford RM, Mann DG (1990) The Diatoms – Biology & Morphology of the genera, Cambridge University Press, Cambridge, pp 728

Stachura-Suchoples K (2001) Bioindicative values of dominant diatom species from the Gulf of Gdansk, Southern Baltic Sea, Poland. In: Jahn R, Kociolek JP, Witkowski A, Compère P (eds) Lange-Bertalot Festschrift. ARG Gantner KG, Ruggell, pp 477-490

van Dam H, Mertens A, Sinkeldam J (1994) A coded checklist and ecological indicator values of freshwater diatoms from the Netherlands. Neth J Aquat Ecol 28:117–133
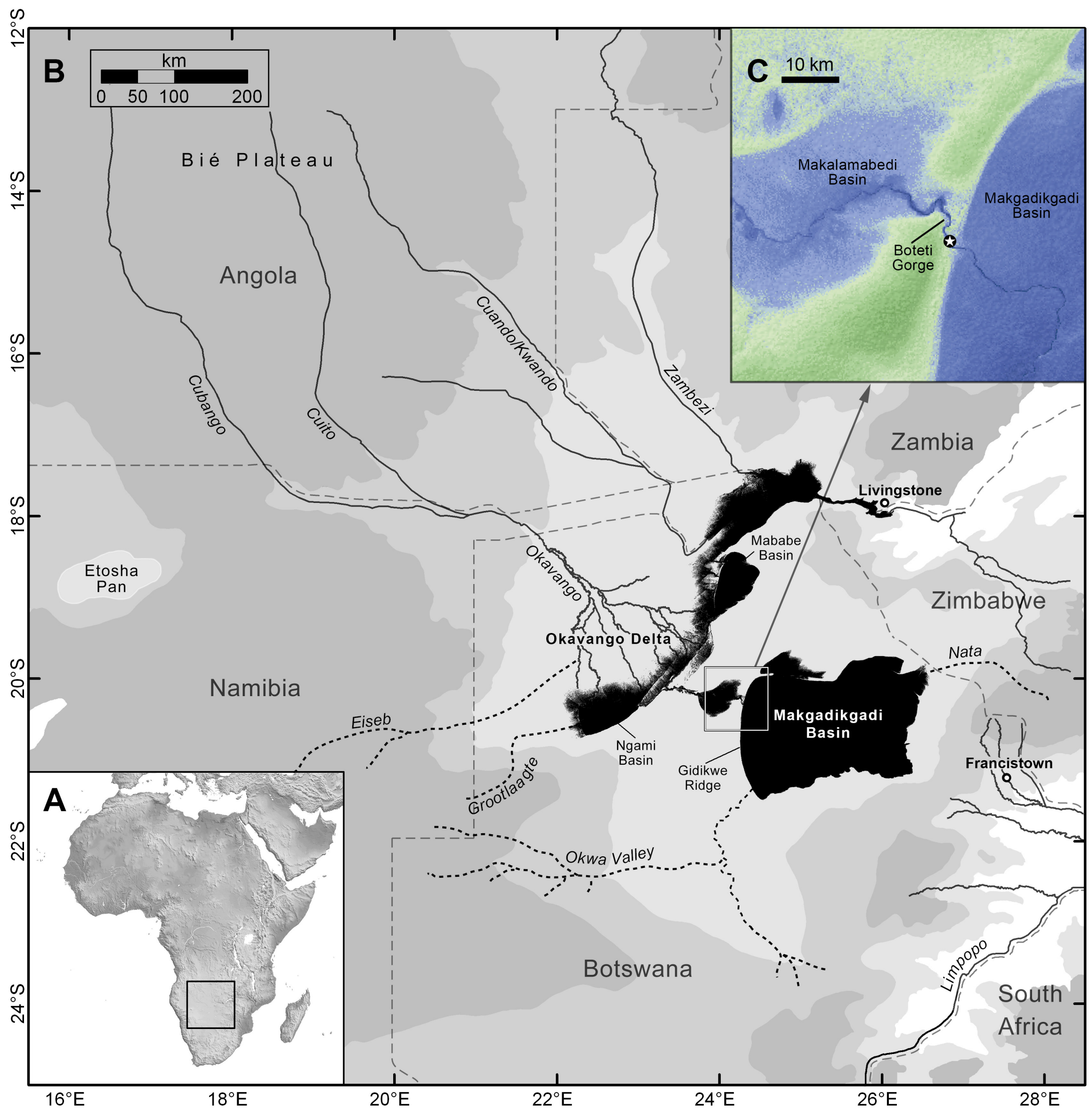
BT1052 / 90.3 ± 9.2 ka

BT885 / 88.5 ± 5.8 ka

BT1054 / 106.3 ± 7.4 ka

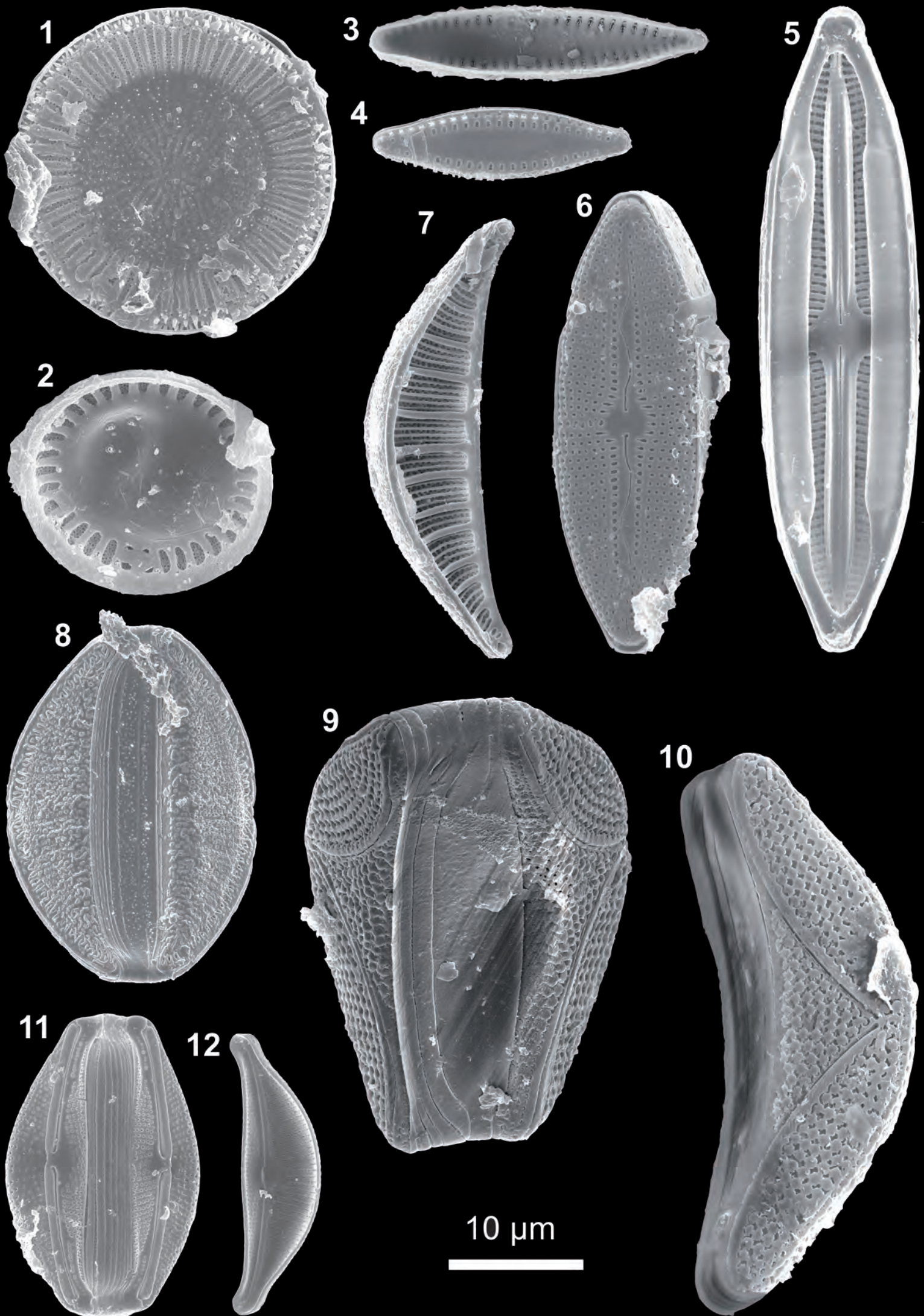BT1055 / 103.4 ± 6.4 ka

30 cm

PLAYA SEDIMENTS

10 µm

Table 1 Analytical data for OSL age calculation: Sample code, ^{238}U, ^{232}Th and ^{40}K-concentrations, total dose rate, equivalent dose and OSL age

Sample	U [ppm]	Th [ppm]	K [%]	$\dot{D}$ [Gy/ka]	D_e [Gy]	OSL Age [ka]
BT 885	1.14 ± 0.08	2.20 ± 0.05	0.41 ± 0.01	0.88 ± 0.04	77.6 ± 3.8	88.5 ± 5.8
BT 1052	0.97 ± 010	2.02 ± 0.04	0.32 ± 0.01	0.66 ± 0.03	59.7 ± 5.2	90.3 ± 9.2
BT 1054	0.91 ± 0.07	2.38 ± 0.05	0.34 ± 0.01	0.69 ± 0.33	72.9 ± 3.7	106.3 ± 7.4
BT 1055	0.93 ± 0.09	2.42 ± 0.05	0.33 ± 0.01	0.68 ± 0.33	70.7 ± 2.8	103.4 ± 6.4

Figure captions

Fig. 1. A. general location of study area. B. Map of Makgadikgadi-Okavango-Zambezi basin (MOZB) of the south-western branch of the East African Rift System and the major tributaries. Black dashed lines indicate valleys of palaeo-rivers. Major subbasins of MOZB shaded black. During late Quaternary hydrologically favourable periods these subbasins may have been part of a mega-lake. Due to tectonics and hydromorphological processes the modern setting can be used only tentatively for simulating past mega-lake sizes and shapes. C. A digital elevation model (modified from Riedel et al. 2014) exhibits the location of the studied geological section at the western edge of the Makgadikgadi Basin where palaeo-shorelines can be found on the structural Gidikwe Ridge.

Fig. 2. Upper part of the Boteti river valley section with studied 30-cm diatom-rich sediment unit on top (BT). Position of samples for OSL dating and OSL dates are indicated.

Fig. 3. Scanning electron microscope images of the six most abundant diatom species identified in the Boteti section top unit (BT). 1-2: *Cyclotella meneghiniana*, 3-4: *Pseudostaurosira brevistriata*, 5-6: *Mastogloia elliptica*, 7-8: *Rhopalodia gibberula*, 9-10: *Epithemia sorex*, 11-12: *Halamphora thermalis*.

Fig. 4. Composite diagram illustrating percentage abundances of most frequent species separated into benthic and planktonic forms, P/B ratio, log-centred PCA, $\delta^{18}O_{diatom}$ variability, and stack diagrams for salinity, trophy and pH inferred from the autecology of the diatom species.